

Undulator test of a Bragg reflection elliptical polarizer at ~ 7.1 keV

S. D. Shastri,^{a)} K. D. Finkelstein, Qun Shen, B. W. Batterman, and D. A. Walko^{b)}
Cornell High Energy Synchrotron Source and the School of Applied and Engineering Physics, Cornell
University, Ithaca, New York 14853

(Presented on 18 July 1994)

A system of diffracting perfect crystals for the generation of variable, elliptically polarized x rays was tested at the Cornell High Energy Synchrotron Source under the conditions of a standard undulator source. The phase retarding optical component was a 4-bounce, Ge(220) Bragg reflection channel-cut crystal. The full polarization state of the output beam, including the circular polarization purity P_3 , was determined using the multiple-beam Bragg diffraction technique. In addition to measuring the optics' efficiency, the ability to scan the system in energy, while frequently reversing the circular helicity, was demonstrated at the vicinity of the Fe K edge at 7.1 keV. The setup was applied to a circular magnetic x-ray dichroism measurement. © 1995 American Institute of Physics.

I. INTRODUCTION

X-ray studies involving scattering or absorption phenomena with complex polarization dependences can sometimes benefit from the use of elliptically polarized x rays. Such phenomena include magnetic scattering, anomalous scattering, nuclear resonance scattering, and circular magnetic x-ray dichroism (CMXD).¹ Primarily, the desire for polarized x rays has come from studies of magnetic materials. As an example, for CMXD, the demands on elliptical polarization producing technology are: circular polarization in particular, with high purity and flux and ease of helicity reversal for cases where sample magnetization reversal is impractical. In addition to the use of off-orbital plane bend magnet radiation and the development of special (helical, elliptical, or asymmetrical) insertion devices² with movable or electrically switchable poles, schemes employing perfect crystal optics have also been researched. Although helicity reversal and broad tunability are not straightforward with the Laue diffraction geometry wave plate, that device is well suited for high x-ray energies and has been used for magnetic Compton scattering studies.³ At lower x-ray energies (6–10 keV) a transmission wave plate in Bragg geometry,⁴ allowing tunability and easy helicity reversal, has been characterized. Here, we report the performance of another device, a multiple-bounce Bragg reflection elliptical polarizer,⁵ under the source conditions of a 3.3 cm period, 123 pole standard undulator at the Cornell high energy synchrotron source (CHESS). The reflection polarizer to be described is conceptually similar to the Fresnel rhomb in classical optics. It exploits the different phase shifts experienced by the mutually orthogonal, linearly polarized σ and π wave fields in dynamical Bragg diffraction. In addition to measuring the full polarization state of the output and the throughput efficiency of the optics, the capabilities of energy scanning and straightforward circular polarization helicity reversal were demonstrated in the neighborhood of the Fe K edge at 7.1 keV.

^{a)}Current address: Advanced Photon Source, Argonne National Laboratory, Argonne, IL 60439.

^{b)}Current address: Physics Department, University of Illinois at Urbana-Champaign, Urbana, IL 61801.

II. PRINCIPLE

Figure 1 shows the σ and π reflectivities and various phase shift quantities in the angular vicinity of the symmetric Ge(220) Bragg reflection at 7.1 keV. For each of the two polarizations σ and π , the phase shift between the incident and diffracted waves undergoes a 180° change over the angular Darwin width. The difference $\phi_{\sigma-\pi}$ between these two curves gives the relative phase retardation between the σ and π wave fields in the generally elliptical diffracted beam that results when the incident beam has a tilted linear polarization, so as to coherently excite both σ and π wave fields. Shifts $\phi_{\sigma-\pi} = \pm 90^\circ$, required for circular polarization, are inaccessible unless one exploits a multiple bounce, channel-cut crystal geometry which extends the range of accumulable phase shift. For a 4-bounce channel cut, a net $\pm 90^\circ$ phase shift is acquired at incident angles θ_L , θ_R where $\phi_{\sigma-\pi} = \pm 90^\circ/4 = \pm 22.5^\circ$, allowing both left and right circular output. Circular light also requires equal σ and π component magnitudes in the output beam. To achieve this, one must compensate for the reflectivity disparity ($R_\sigma/R_\pi > 1$) and fa-

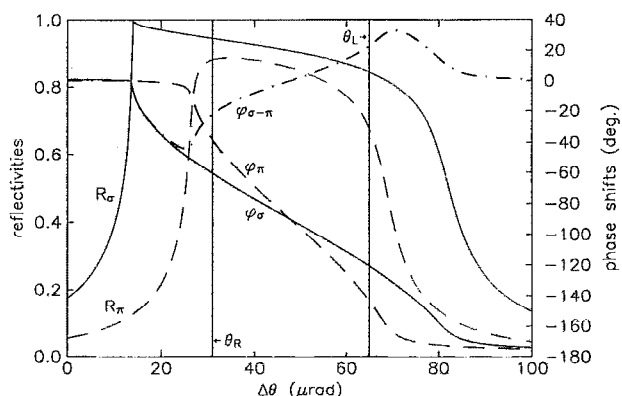


FIG. 1. Calculated reflectivities R_σ, R_π and phase shifts for 1 bounce, sym. Ge(220) at 7.1 keV as functions of angular deviation from the kinematical Bragg angle θ_B . The phase shift between the incident and diffracted waves for the $\sigma(\pi)$ polarization is ϕ_σ (ϕ_π). The difference $\phi_{\sigma-\pi} = \phi_\sigma - \phi_\pi$ is the 1-bounce phase retardation.

vor the π polarization by preparing the incident linear plane of polarization to be tilted at $\chi \approx 53^\circ$ from the σ axis. To reduce phase smearing and the consequent polarization impurity, the incident beam divergence must be made smaller than the rocking curve widths involved. The feasibility of this scheme is optimal in the 6–10 keV x-ray energy range.

III. OPTICS

The experimental setup is shown in Fig. 2. The x rays incident on the 4-bounce were linearly prepolarized by a Si(331) channel-cut ($2\theta_B \sim 90^\circ$) rotated by the desired tilt angle $\chi = 53^\circ$. The parallel channel reflecting surfaces were cut to an acceptance-widening asymmetry angle of 22° to gather more vertical and horizontal rays. Ideally, immediately upstream of this prepolarizer, one would want a Si(220)/Ge(220) double-crystal monochromator (with the Ge crystal asymmetrically cut for output collimation) so as to maintain a nondispersive geometry with the 4-bounce; matched d spacings are crucial to avoid drastic degradation of the polarization purity. However, due to the unavailability of a high heat load Si(220) monochromator crystal, a Si(111)/Si(111) monochromator (not shown) was used. The nondispersion requirement was met with a compensating asymmetric-symmetric Si(220) channel-cut which collimated the beam to an acceptable vertical divergence of $12 \mu\text{rad}$, in addition to transforming its DuMond (λ vs θ dispersion) profile to the desired form. This crystal, called the collimator, had only its first reflecting surface miscut with an asymmetry factor $b = -1/6$.

IV. POLARIZATION MEASUREMENT AND EFFICIENCY RESULTS

The Stokes–Poincaré polarization parameters (P_1, P_2, P_3) of the beam after the 4-bounce were determined for various fixed angles on its reflection curve using the multiple-beam diffraction technique⁶ (described elsewhere in this volume). The results at 7.070 keV are compared in Fig. 3 to dynamical calculations, showing acceptable agreement. The calculations include the $12 \mu\text{rad}$ vertical divergence broadening, whose effect on the circular polarization purity P_3 is to reduce it from the ideal ± 1 values to ± 0.85 . Circular helicity reversal is achieved simply by a $30 \mu\text{rad}$ angular rotation of the 4 bounce. Repeating these polarization measurements ~ 100 eV higher in photon energy (i.e., at 7.160 keV) gave the same results.

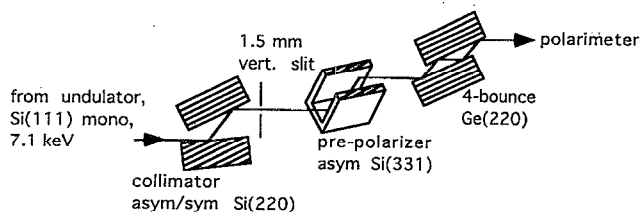


FIG. 2. Optics: the “collimator” is unnecessary if the proper (220) monochromator is used.

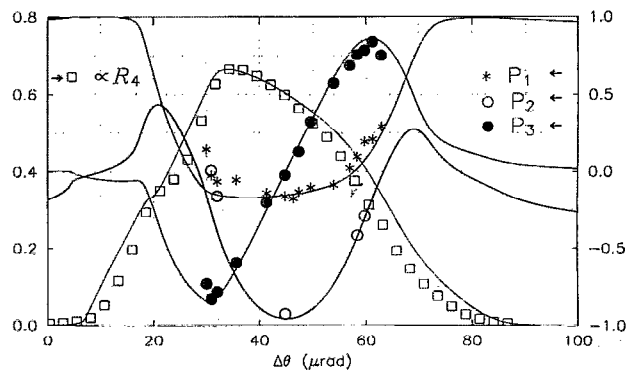


FIG. 3. Results at 7.070 keV for the 4-bounce reflectivity R_4 and output polarization parameters (P_1, P_2, P_3). Lines are dynamical calculations which include the $12 \mu\text{rad}$ angular divergence broadening.

Optimal production of right circular x rays is predicted when all crystals are set for close to peak reflectivity. In this configuration, the calculated flux throughput efficiencies of the collimator, prepolarizer, and 4 bounce are 76%, 6%, and 66%, respectively. The collimator and prepolarizer efficiency estimates assume undulator x-ray emittance angles measured in the first dedicated undulator run (1988):⁷ $40 \mu\text{rad}$ vertical, $100 \mu\text{rad}$ horizontal. The overall predicted efficiency of the system is the product 3%. The measured efficiency was 1% after correction for the air absorption path (1 m, $e^{-\mu t} \approx 0.2$) and the slit aperture (Fig. 2) immediately downstream of the collimator, which cut down the vertical size and flux of the beam by a factor of 5. This slitting down was done because the collimator blew up, by the factor $1/|b|=6$, the vertical beam size to a dimension that was too large for accommodation by the 4-bounce crystal gap and length. Investigating this efficiency discrepancy revealed that the individually measured efficiencies for the collimator, prepolarizer, and 4-bounce were 0.65, 0.54, and 0.86 of their respective predicted values. Confidence, based on other tests, in the crystal quality of the collimator and prepolarizer leads us to question the undulator divergence values used. However, the less than expected 4-bounce peak reflectivity is most likely due to a slight strain imperfection in the Ge, which could also explain the measured 4-bounce rocking curve being narrower than calculated (Fig. 3). The raw experimental efficiency, uncorrected for air absorption and the aperturing, as much less than 1%. At a 90 mA e^- current, a photon flux of 6×10^{11} Hz incident on the collimator resulted in a 3×10^8 Hz output of right circular flux from the 4-bounce in a beam of dimensions 5 mm (horiz.), 1.5 mm (vert.), and energy resolution slightly less than 1 eV.

V. CMXD

Circular magnetic x-ray dichroism (CMXD) was attempted at the vicinity of the Fe K edge (7.112 keV) by placing a sample after the 4-bounce. All optical components were scanned together in energy, with transmission data measured for both helicities at every energy step of the scan. In looking for a dichroic signal in the CMXD profile [$\Delta\mu(E) = \mu_{\text{left}} - \mu_{\text{right}}$], features appeared which did not

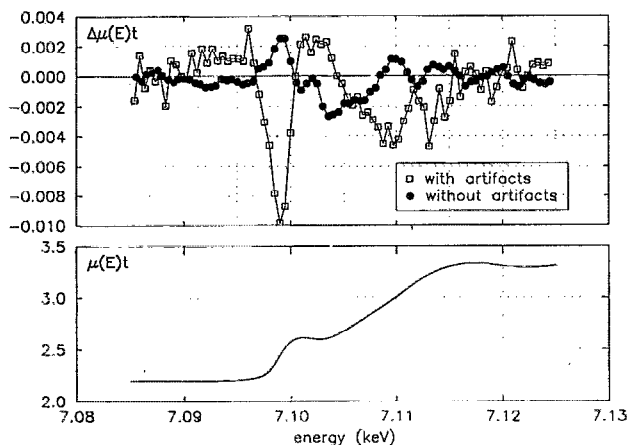


FIG. 4. Fe *K*-edge CMXD profiles for $\text{Pr}_2\text{Fe}_{14}\text{B}$ with and without the energy shift related artifacts, whose dips occur at edge inflection points. These data were accumulated over a few hours.

change sign upon reversal of the sample magnetization. These features, superimposed on the true CMXD profile, are due to a small energy shift $\delta E \approx 0.05$ eV that arises when the 4-bounce alone rotates from the left to the right circular angle. This energy shift contaminates the CMXD profile with artifacts $-\delta E d\mu(E)/dE$ related to the derivative of the edge jump. Figure 4 shows CMXD profiles, both with and without the artifact, for a thin, premagnetized $\text{Pr}_2\text{Fe}_{14}\text{B}$ single-domain powder sample. Removal of the artifact (which is larger than the signal for this sample) was attempted here by subtracting two CMXD spectra taken with opposite magnetizations.

The reason the shift δE , despite the incident beam on the 4-bounce being unchanged, is the following: in going from the left to the right circular point of the rocking curve, the reflectivity weightings for the different energy slices of the DuMond profile of the incident beam undergo changes that shift the energy spectrum centroid by 0.05 eV. The energy shift is avoided (and $|P_3|$ values close to 1 result) if one were to eliminate the collimator and replace the Si(111)/Si(111) monochromator with Si(220)/asym.Ge(220), as mentioned earlier.

VI. CONCLUDING REMARKS

In addition to the above suggestion, one can enhance the performance of the optics with other improvements. Air absorption, if significant, is often easily remedied. The undulator source used had x-ray divergences which, although smaller than that of typical bend magnet sources, is considerably larger than that of more recently constructed and planned insertion devices in various synchrotron facilities. A smaller horizontal divergence would increase the throughput

of the tilted prepolarizer. A smaller vertical divergence would allow a less asymmetric cut for the collimating monochromator crystal while preserving the polarization purity. This, combined with a smaller initial beam size, would result in less or no flux loss from slitting the blowup, collimated beam. With these changes and judicious choice of asymmetric cuts, the efficiency of the entire system could surpass the 10% level and result in $|P_3|$ values close to 1.

The multiple-bounce polarizer optical element is more efficient than a Bragg transmission wave plate⁴ of Si by a factor of 2–4. However, transmission wave plates of diamond can have much higher efficiencies. Furthermore, the latter scheme has the significant advantage of being less demanding on crystal perfection and on incident angular collimation, making it especially attractive when $|P_3|$ values close to 1 are not crucial. The Bragg transmission plate's relative insensitivity to divergence better suits it to energy dispersive geometries for the simultaneous collection of CMXD data over a wide energy range. The two methods are comparable in helicity reversal ease and tunability.

The ability to scan the Bragg reflection polarizer optics in energy, with frequent left/right circular helicity reversals, has been demonstrated at the vicinity of the Fe *K* edge at 7.1 keV. The existence of artifacts in circular dichroism data, due to a subtly arising 0.05 eV energy shift, suggests an important consideration in crystal polarization optics design for CMXD applications. At a small enough level, a shift is always likely to exist and poses a problem only if the dichroic signal is sufficiently weak, as in our case. The appropriate monochromator would have removed most of the energy shift here.

We thank J. LaLuppa for software implementation of the energy scanning and helicity reversal, W. Capehart for providing the $\text{Pr}_2\text{Fe}_{14}\text{B}$ sample, and M. Bedzyk for his valuable participation in an early experiment done with a bend magnet source. The assistance of J. White, P. Doing, and the rest of the CHESS staff is appreciated. CHESS is supported by the National Science Foundation under Award No. DMR 93-11772.

¹G. Schütz, W. Wagner, W. Wilhelm, P. Kienle, R. Zeller, R. Frahm, and G. Materlik, *Phys. Rev. Lett.* **58**, 737 (1987).

²H. Kitamura, *Synch. Rad. News*, **5**, 14 (1992).

³M. Hart, *Philos. Mag. B* **38**, 41 (1978); D. Mills, *Phys. Rev. B* **36**, 6178 (1987).

⁴V. Belyakov and V. Dmitrienko, *Sov. Phys. Uspek.* **32**, 697 (1989); K. Hirano, K. Izumi, T. Ishikawa, S. Annaka, and S. Kikuta, *Jpn. J. Appl. Phys.* **30**, 407 (1991).

⁵B. Batterman, *Acta. Cryst. Suppl. A* **40** (1984); B. Batterman, *Phys. Rev. B* **45**, 12677 (1992). Related work on Bragg case polarization: O. Brümmer, Ch. Eisenschmidt, and H. Höche, *Acta. Cryst. A* **40**, 394 (1984).

⁶Q. Shen and K. Finkelstein, *Phys. Rev. B* **45**, 5075 (1992); Q. Shen, S. Shastri, and K. Finkelstein (these proceedings).

⁷D. Bilderback *et al.*, *Rev. Sci. Instrum.* **60**, 1419 (1989).